NASA Technical Memorandum 105555

Effect of Liquid Surface Turbulent Motion on the Vapor Condensation in a Mixing Tank

P.14

C.S. Lin
Analex Corporation
Brook Park, Ohio

and

M.M. Hasan
Lewis Research Center
Cleveland, Ohio

Prepared for the
Fourth International Symposium on Transport Phenomena
in Heat and Mass Transfer
sponsored by the University of New South Wales
Sydney, Australia, July 14-19, 1991

NASA

EFFECT OF LIQUID SURFACE TURBULENT MOTION ON THE VAPOR CONDENSATION IN A MIXING TANK

C.S. Lin
Analex Corporation
Brook Park, Ohio 44142

and

M.M. Hasan
National Aeronautics and Space Administration
Lewis Research Center
Cleveland, Ohio 44135

ABSTRACT

The effect of liquid surface motion on the vapor condensation in a tank mixed by an axial turbulent jet is numerically investigated. The average value (over the interface area) of the root-mean-squared (rms) turbulent velocity at the interface is shown to be linearly increasing with decreasing liquid height and increasing jet diameter for a given tank size. The average rms turbulent velocity is incorporated in Brown et al. (1990) condensation correlation to predict the condensation of vapor on a liquid surface. The results are in good agreement with available condensation data.

1. INTRODUCTION

The interface condensation process which is principally controlled by liquid motion in a partially filled tank is of interest to space-based systems. In space environment, a preferred method to control cryogenic storage tank pressure is the use of jet-induced mixing (Aydelott, et al., 1985; Poth and Van Hook, 1972). For a laminar jet the interface condensation rate could be simply determined by the jet volume flow rate and jet subcooling (Lin, 1989; Hasan and Lin, 1990; and Lin and Hasan, 1990). However, the space-based systems are dimensionally large. The axial jet mixing system in most applications will be turbulent. Sonin et al. (1986); Brown et al (1989); and Brown et al. (1990) obtained an empirical correlation for the rate at which a pure vapor condenses on the free surface of a turbulent liquid in a steam-water system, for conditions where buoyancy effects are insignificant.

Figure 1 shows the physical system and the coordinates similar to that used in Brown and Sonin's steam-water condensation experiments (Sonin, et al., 1986; Brown, et al., 1989). The system consists of a vertical cylindrical tank of diameter D, partially filled with water. A steady turbulence is created in the water by an axial jet which is directed toward

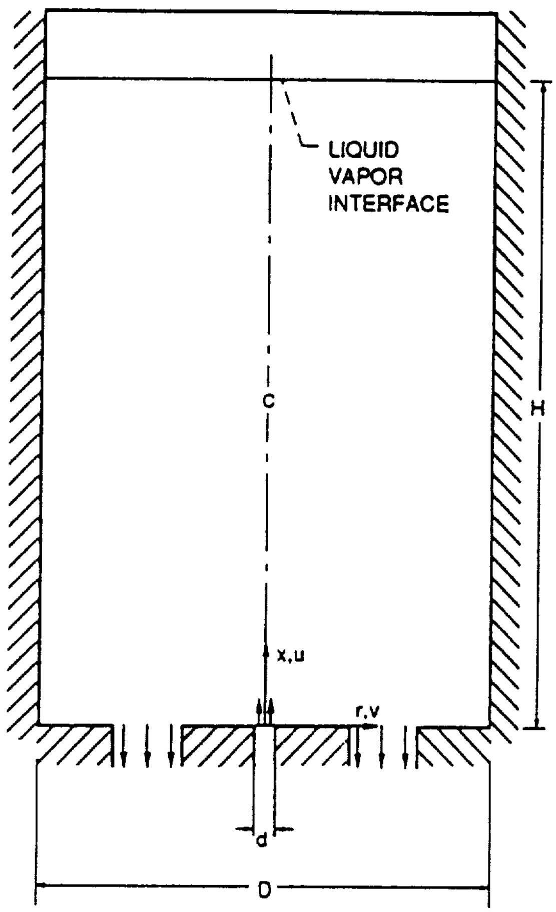

FIGURE 1. Physical system and coordinates.

the free surface from below, with the water circulating in a closed loop (not shown here) through a pump and cooler. Thus, a certain degree of subcooled axial jet flow can be maintained to induce vapor condensation at the surface. It was shown by Brown et al. (1990) that, for high jet submergence $H/D > 3.1$ and at conditions where buoyancy effect are insignificant, the condensation mass flux m_c of the pure vapor at the turbulent surface of its liquid is given by

$$St_c = 0.0198\left(1 - \frac{Ja}{2}\right)Pr^{-0.33} \tag{1}$$

The condensation Stanton number is based on the condensation heat flux ($m_c h_{fg}$), the local bulk liquid subcooling ($T_s - T_{out}$), and the local rms value of turbulent velocity (v_s') extrapolated from the bulk to the surface. For high jet submergence range $3.1 < H/D < 4.2$, a correlation for the average value of rms turbulant velocity over the interface, $\overline{v_s'}$, was given by Brown et al. (1990):

$$\overline{v_s'} = 21.1\left(\frac{Q_j}{Dd}\right)e^{-1.2H/D} \tag{2}$$

Brown et al. (1989) also conducted experiments to measure the mass condensation rate for jet submergence range $0.5 < H/D < 3$. However, the turbulence intensity was not measured. Following Thomas (1979), they modeled the interfacial turbulence intensity distribution and obtained an expression for the average value of v_s' over the interface as

$$\overline{v_s'} = \frac{u_j\, d}{D}\left[10.4\beta_2 - \left(7.14\beta_2 - 3.06\beta_1\right)\frac{H}{D}\right] \tag{3}$$

where β_1 and β_2 are constants to be determined. Assuming Eq. (1) also applies to the low jet submergence, the condensation data of Brown et al. (1989) yield

$$\beta_1 = 0.34 \qquad \beta_2 = 0.24 \tag{4}$$

The purpose of this study is to numerically determine the value of $\overline{v_s'}$ by exactly solving for the entire flow field in a tank with $0.5 < H/D < 3$. The liquid-side turbulence as a function of relevant parameters is determined and incorporated in Eq. (1) to predict the vapor condensation rate and compared with the experimental data of Brown et al. (1989).

2. PROBLEM FORMULATION AND MATHEMATICAL MODELING

The physical system and coordinates are shown in Fig. 1. An axial liquid jet of diameter d and of velocity u_j, located at the tank bottom, is continuously introduced into the tank along the tank centerline. Liquid is withdrawn from the outer portion of the tank bottom with a withdrawing area of A_{out}. The volume flow rate of the liquid withdrawn is the same as that of the injected liquid jet such that the liquid level height H of the tank (or jet submergence) is maintained constant. The effect of vapor motion on the liquid turbulence is assumed negligible. Also the liquid surface is assumed to be flat.

The jet-induced mixing problem considered in the present study is steady-state and incompressible with gravity acting in the vertical negative-x direction. The dimensionless form of continuity and momentum equations with K-ε turbulence model are expressed as

$$\frac{\partial u^*}{\partial x^*} + \frac{1}{r^*}\frac{\partial (r^* v^*)}{\partial r^*} = 0 \tag{5}$$

$$\frac{\partial(u^{*2})}{\partial x^*} + \frac{\partial(u^* r^* v^*)}{r^* \partial r^*} = -\frac{\partial p^*}{\partial x^*} + \frac{\partial}{\partial x^*}\left[\left(\frac{1}{B\ Re_j} + \frac{C_u K^{*2}}{\varepsilon^*}\right)\frac{\partial u^*}{\partial x^*}\right] + \frac{\partial}{r^* \partial r^*}$$

$$\left[\left(\frac{1}{B\ Re_j} + \frac{C_u K^{*2}}{\varepsilon^*}\right) r^* \frac{\partial u^*}{\partial r^*}\right] + \frac{\partial}{\partial x^*}\left[\left(\frac{1}{B\ Re_j} + \frac{C_u K^{*2}}{\varepsilon^*}\right)\frac{\partial u^*}{\partial x^*} - \frac{2}{3} K^*\right]$$

$$+ \frac{\partial}{r^* \partial r^*}\left[\left(\frac{1}{B\ Re_j} + \frac{C_u K^{*2}}{\varepsilon^*}\right) r^* \frac{\partial v^*}{\partial r^*}\right] \qquad (6)$$

$$\frac{\partial(u^* v^*)}{\partial x^*} + \frac{\partial(r^* v^{*2})}{r^* \partial r^*} = -\frac{\partial p^*}{\partial r^*} + \frac{\partial}{\partial x^*}\left[\left(\frac{1}{B\ Re_j} + \frac{C_u K^{*2}}{\varepsilon^*}\right)\frac{\partial v^*}{\partial x^*}\right] + \frac{\partial}{r^* \partial r^*}$$

$$\left[\left(\frac{1}{B\ Re_j} + \frac{C_u K^{*2}}{\varepsilon^*}\right) r^* \frac{\partial v^*}{\partial r^*}\right] + \frac{\partial}{\partial x^*}\left[\left(\frac{1}{B\ Re_j} + \frac{C_u K^{*2}}{\varepsilon^*}\right)\frac{\partial u^*}{\partial r^*}\right] + \frac{\partial}{r^* \partial r^*}$$

$$\left[\left(\frac{1}{B\ Re_j} + \frac{C_u K^{*2}}{\partial^*}\right) r^* \frac{\partial v^*}{\partial r^*} - \frac{2}{3} r^* K^*\right] - \left(\frac{1}{B\ Re_j} + \frac{C_u K^{*2}}{\varepsilon^*}\right)\frac{2 v^*}{r^{*2}} \qquad (7)$$

$$\frac{\partial(u^* K^*)}{\partial x^*} + \frac{\partial(K^* r^* v^*)}{r^* \partial r^*} = \frac{\partial}{\partial x^*}\left[\left(\frac{1}{B\ Re_j} + \frac{C_u K^{*2}}{\sigma_K \varepsilon^*}\right)\frac{\partial K^*}{\partial x^*}\right]$$

$$+ \frac{\partial}{r^* \partial r^*}\left[\left(\frac{1}{B\ Re_j} + \frac{C_u K^{*2}}{\varepsilon^*}\right) r^* \frac{\partial K^*}{\partial r^*}\right] + \left(\frac{1}{B\ Re_j} + \frac{C_u K^{*2}}{\varepsilon^*}\right) G - \varepsilon^* \qquad (8)$$

$$\frac{\partial(u^* \varepsilon^*)}{\partial x^*} + \frac{\partial(\varepsilon^* r^* v^*)}{r^* \partial r^*} = \frac{\partial}{\partial x^*}\left[\left(\frac{1}{B\ Re_j} + \frac{C_u K^{*2}}{\sigma_\varepsilon \varepsilon^*}\right)\frac{\partial \varepsilon^*}{\partial x^*}\right] + \frac{\partial}{r^* \partial r^*}$$

$$\left[\left(\frac{1}{B\ Re_j} + \frac{C_u K^{*2}}{\sigma_\varepsilon \varepsilon^*}\right) r^* \frac{\partial \varepsilon^*}{\partial r^*}\right] + \left(\frac{1}{B\ Re_j} + \frac{C_u K^{*2}}{\varepsilon^*}\right) G C_1 \frac{\varepsilon^*}{K^*} - C_2 \frac{\varepsilon^{*2}}{K^*} \qquad (9)$$

where the turbulence production term, G, is defined as

$$G = 2\left[\left(\frac{\partial u^*}{\partial x^*}\right)^2 + \left(\frac{\partial v^*}{\partial r^*}\right)^2 + \left(\frac{v^*}{r^*}\right)^2\right] + \left(\frac{\partial u^*}{\partial r^*} + \frac{\partial v^*}{\partial x^*}\right)^2 \tag{10}$$

and the empirical constants associated with the turbulence model are

$$C_1 = 1.44, \quad C_2 = 1.92, \quad \text{and} \quad C_u = 0.09 \tag{11}$$

Boundary conditions are required to solve the partial differential Eqs. (5) to (9). At the centerline, the symmetric conditions are used. No-slip conditions for velocities are applied at the solid walls. Wall functions (Launder and Spalding, 1974) are used to calculate shear stress and are included as a source term in the governing equation for the velocity component parallel to the wall. For the axial jet, uniform velocity is assumed. The turbulent kinetic energy of the jet is set to be uniform at a specified level. The distribution of the dissipation rate is given by

$$\varepsilon_j^* = C_u^{3/4} \frac{K_j^{*3/2}}{l_m/D} \tag{12}$$

where l_m is the mixing length scale (Escudier, 1966).

Uniform velocity at the liquid-withdrawn plane is also assumed:

$$u_{out}^* = -\frac{A_j}{A_{out}} \quad \text{and} \quad v_{out}^* = 0 \tag{13}$$

At the free surface, zero axial velocity and shear-free conditions are used:

$$u_s^* = 0 \quad \text{and} \quad \left(\frac{\partial v^*}{\partial x^*}\right)_s = 0 \tag{14}$$

Net fluxes of turbulent quantities K^* and ε^* are assumed zero at the free surface and liquid withdrawn-plane:

$$\left(\frac{\partial K^*}{\partial x^*}\right)_s = \left(\frac{\partial \varepsilon^*}{\partial x^*}\right)_s = 0 \quad \text{and} \quad \left(\frac{\partial K^*}{\partial x^*}\right)_{out} = \left(\frac{\partial \varepsilon^*}{\partial x^*}\right)_{out} = 0 \tag{15}$$

The governing equations are numerically solved by a finite-difference method. Nonuniform grid distribution is used with concentration of the grid nodes in the centerline, near-wall, and near-interface regions where the gradients of flow properties are expected to be large. The essential features of the numerical scheme are described in Lin (1989) and Lin and Hasan (1990).

The grid patterns of 60 by 41 and 84 by 41 have been shown to give reasonably grid-independent solutions for $Ar \leq 1$ and $2.5 \geq Ar > 1$, respectively. The convergent solutions are considered to be reached when the maximum of absolute residual sums for u*, v*, and K* variables is less than 10^{-6}. In the present study, calculations are performed to cover a wide range of the parameters Re_j, D/d and Ar: $10\ 000 \leq Re_j \leq 60\ 000$, $15 < D/d < 70$, and $0.5 \leq H/D \leq 2.5$. The value of K_j^* is fixed at 0.005 and $A_{out}/A_j = 80$.

3. RESULTS AND ANALYSIS

The effects of the jet Reynolds number (Re_j), aspect ratio (Ar) and tank to jet diameter ratio (D/d) on the turbulent quantities at and near the interface are of particular interest. Numerical solutions show that the dimensionless turbulent kinetic energy distribution (K*) at the interface is slightly increasing with Re_j. However, this increase is so insignificant that the average value of $\bar{K}_s^*$ over the interface is essentially independent of Re_j as shown in Fig. 2. Figure 3 shows the distribution of dimensionless turbulent kinetic energy at the interface (K_s^*) as a function of aspect

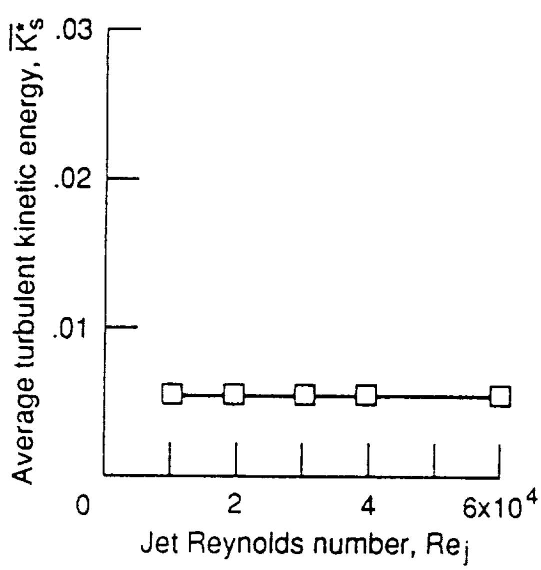

FIGURE 2. Average turbulent kinetic energy at the interface as a function of jet Reynolds number (H/D = 0.967, D/d = 23.6).

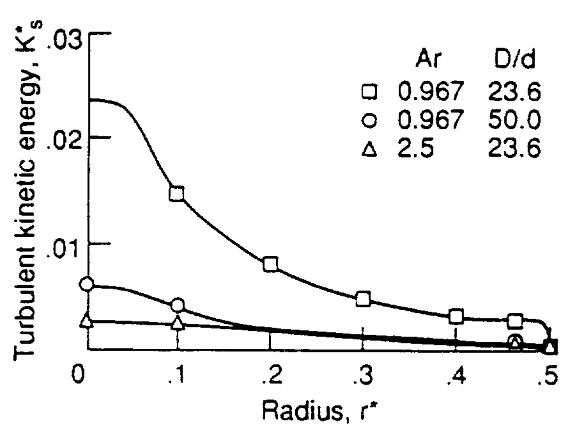

FIGURE 3. Effects of tank aspect ratio and tank to jet diameter ratio on the turbulent kinetic energy at the interface (Re_j = 20 000).

ratio, Ar, and tank to jet diameter ratio, D/d. An increase in either Ar or D/d results in a lower level of turbulent kinetic energy at the interface. This is because, for greater Ar or D/d, more energy is dissipated and less energy remains when the interface is reached. Also, greater values of Ar and D/d yield more uniform radial distribution of K_s^*. For Ar greater than 3, the rms turbulent velocities were found to be nearly uniform at and near the interface (Sonin et al., 1986).

Komori et al. (1982) measured the turbulence intensities, i.e., rms values of three components of velocity fluctuations, in an open channel flow. It was observed that near the free surface, the intensity of vertical fluctuation decreases while the fluctuations parallel to the surface are promoted. This behavior has also been observed by Sonin et al. (1986) in a flow system similar to Fig. 1. At the interface, since the axial component of fluctuating velocity is damped out, only radial and circumferential turbulent velocities contribute to the turbulent kinetic energy. From the measurements of Komori et al. (1982), it can be seen that the turbulent intensities parallel to the free surface are nearly equal at the free surface. Thus, for an open channel flow, the rms value of the turbulent velocity at the free surface is approximately equal to the square-root of its turbulent kinetic energy. The average value of $v_s'^*$ over the interface can be calculated by

$$\overline{v_s'^*} = 8\int_0^{0.5} v_s'^* r^* \, dr^* = 8\int_0^{0.5} K_s^{*1/2} r^* \, dr^* \tag{16}$$

However, for the axial jet problem in the present study, the two components of interfacial turbulent velocity in the direction parallel to the interface may be significantly different. This observation is based on the experiments of a turbulent radial wall jet performed by Poreh et al. (1967). Therefore, the averaging process of Eq. (16) may not be appropriate. An alternative is to calculate the average value of the dimensionless turbulent kinetic energy over the interface by

$$\overline{K_s^*} = 8\int_0^{0.5} K_s^* r^* \, dr^* \tag{17}$$

and obtain the average value of rms dimensionless turbulent velocity by

$$\overline{v_s'^*} = \overline{K_s^*}^{1/2} \tag{18}$$

Equation (18) can be considered as a system value of rms dimensionless turbulent velocity at the interface and is used as the definition of $\overline{v_s'^*}$ in the present study. It is noted that if the distribution of K_s^* is uniform, Eqs. (16) and (18) should give the same value of $\overline{v_s'^*}$.

Figures 4 and 5 show that $\overline{v_s'^*}$ is decreasing with increasing D/d and Ar, respectively. Based on the numerical solutions, a correlation is obtained for the average value of rms interfacial turbulent velocity ($\overline{v_s'^*}$):

$$\overline{v_s'^*} = (2.39 - 0.645\ Ar)\left(\frac{D}{d}\right)^{-1} \tag{19}$$

for $0.5 \leq Ar \leq 2.5$ and $15 < D/d < 70$. Within this range, $\overline{v_s'^*}$ is essentially a linear function of d/D and Ar. For a given tank size (D), the value of $\overline{v_s'^*}$ is linearly increasing with increasing jet diameter (d) and decreasing liquid height (H).

The value of $\overline{v_s'}$ $(= u_j \overline{v_s'^*})$ is the turbulent quantity required in Brown et al. (1990) condensation rate correlation. The average condensation mass flux at the surface can be obtained by integrating Eq. (1) and is expressed as:

$$\overline{\dot{m}_c}\, h_{fg} = \rho C_p \overline{St_c}(T_s - T_{out})\overline{v_s'} \tag{20}$$

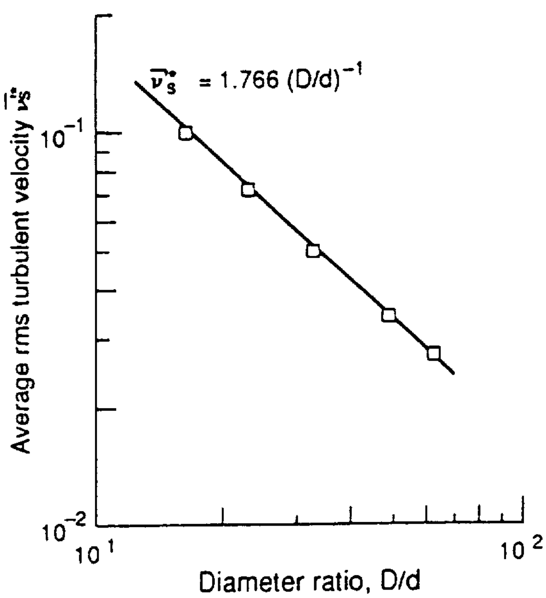

FIGURE 4. Effect of tank to jet diameter ratio on the average rms turbulent velocity at the interface (Re_j = 30 000, H/D = 0.967).

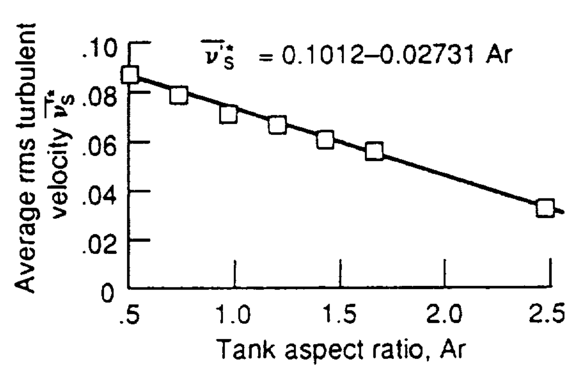

FIGURE 5. Effect of tank aspect ratio on the average rms turbulent velocity at the interface (Re_j = 20 000, D/d = 23.6).

Substituting Eqs. (1) and (19) into Eq. (20), the dimensionless system condensation rate (Π) becomes

$$\Pi = 0.0602 - 0.0163 \frac{H}{D} \tag{21}$$

where $\Pi = \overline{m_c}\, h_{fg}\, D\, d\, Pr^{0.33}/[\rho C_p Q_j (T_s - T_{out})(1 - Ja/2)]$ as defined in Brown et al. (1989). Figure 6 shows good agreement between the measurement of Brown et al. (1989) and Eq. (21). Therefore, Eq. (21), based on the definition of Eq. (18) to predict $v_s'^*$ can be incorporated with Brown et al. (1990) condensation correlation for the condensation rate of a vapor with low jet submergence. Based on Eq. (19), the corresponding values of β_1 and β_2 for Eq. (3) are given by

$$\beta_1 = 0.33 \quad \text{and} \quad \beta_2 = 0.23 \tag{22}$$

which is in very good agreement with Eq. (4) in the model of Brown et al. (1989).

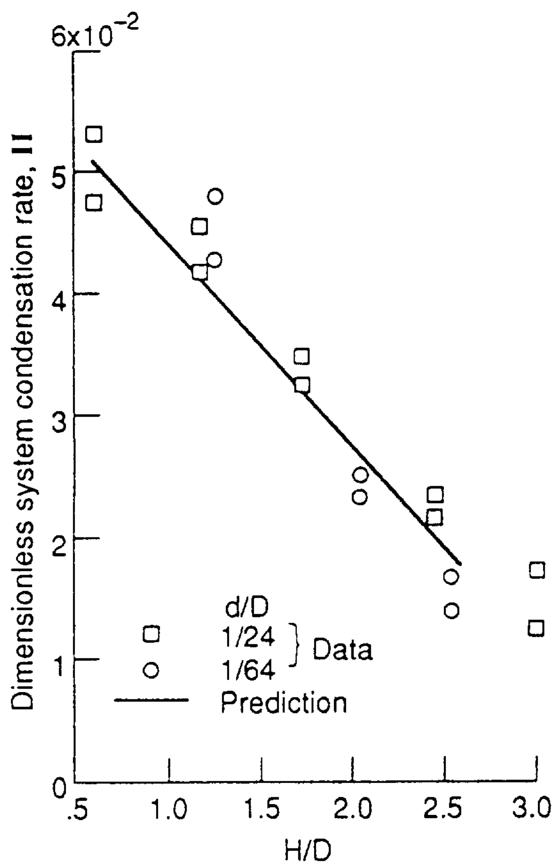

FIGURE 6. Comparison of Eq. (21) and Experimental data of Brown et al. (1989).

4. CONCLUSIONS

For an axial jet-induced mixing system as shown in Fig. 1, numerical calculations based on the assumptions and ranges of parameters considered lead to the following conclusions:

o The radial distribution of turbulent kinetic energy at the interface (K_s) is more uniform for greater Ar and D/d with the maximum value located at the centerline. The average value of dimensionless turbulent kinetic energy over the interface is essentially independent of jet Reynolds number (Re_j) and decreases with increasing aspect ratio (Ar) and tank to jet diameter ratio (D/d). However, experimental data are required for further quantitative evaluation.

o The average (system) value of rms turbulent velocity ($v_s'^*$) over the interface is linearly increasing with decreasing Ar and (D/d) for $0.5 \leq Ar \leq 2.5$ and $15 < D/d < 70$. Equation (19) for the prediction of $\overline{v_s'}$ can be incorporated with Brown et al. (1990) condensation correlation (Eq. (1)), for the vapor condensation rate in a tank mixed by an axial turbulent jet.

NOMENCLATURE

A_j, A_{out}	surface area of the jet and outflow
Ar, B	aspect ratio, H/D, tank to jet diameter ratio, D/d
C_p	specific heat at constant pressure
d, D	jet diameter, tank diameter
g	acceleration due to gravity
H	jet submergence depth
h_{fg}	latent heat of condensation
Ja	Jakob number, $C_p(T_s - T_{out})/h_{fg}$
K^*	dimensionless turbulent K.E., $K^* = K/u_j^2$
l_m	mixing length scale
m_c	local condensation mass flux
Pr	Prandtl number of bulk liquid
p, p_g	pressure, equilibrium hydrostatic pressure
p^*	dimensionless pressure, $p^* = (p - p_g)/(\rho u_j^2)$
Q_j	jet volume flow rate
r^*	dimensionless radial coordinate, r/D
Re_j	jet Reynolds number, $\rho u_j\, d/\mu$
St_c	local condensation Stanton number, $m_c h_{fg}/[\rho C_p (T_s - T_{out}) v_s']$

T_j, T_{out}, T_s — temperature of the jet, outflow, and interface, respectively

u^* — dimensionless axial mean velocity, u/u_j

v^* — dimensionless radial mean velocity, v/u_j

v' — rms turbulent velocity

v'^* — dimensionless rms turbulent velocity, v'/u_j

x^* — dimensionless axial coordinate, x/D

Greek symbols

ε^* — dimensionless dissipation rate of turbulent kinetic energy, $\varepsilon/(u_j^3/D)$

Π — dimensionless system condensation rate

μ — dynamic viscosity

β_1, β_2 — empirical constants in Eq. (3)

ρ — liquid density

σ_K — Prandtl number in K equation, $\sigma_K = 1.0$

σ_ε — Prandtl number in ε equation, $\sigma_\varepsilon = 1.23$

Subscripts

j — evaluated at jet inlet

out — evaluated at outflow location

s — evaluated at liquid-vapor interface

5. REFERENCES

Aydelott, J.C., Carney, M.J., and Hochstein, J.I., NASA Lewis Research Center Low-Gravity Fluid Management Technology Program. NASA TM-87145, 1985.

Brown, J.S., Helmick, M.R., and Sonin, A.A., Vapor Condensation at a Turbulent Liquid Surface in Systems with Possible Space-Based Applications. AIAA Paper 89-2846, July 1989.

Brown, J.S., Khoo, B.C., and Sonin, A.A., Rate Correlation for Condensation of Pure Vapor on Turbulent, Subcooled Liquid. Int. J. Heat Mass Trans., vol. 33, no. 9, pp. 2001-2018, 1990.

Escudier, M.P., Distribution of Mixing Length in Turbulent Flows Near the Walls. Report TWF/TN/1, Imperial College of Science and Technology, Dept. of Mech. Engr., London, U.K., 1966.

Gibson, M.M., and Rodi, W., Simulation of Free Surface Effects on Turbulence with a Reynolds Stress Model. J. Hydraulic Research, vol. 27, no. 2, pp. 233-244, 1989.

Hasan, M.M., and Lin, C.S., Buoyancy Effects on the Vapor Condensation Rate on a Horizontal Liquid Surface. AIAA Paper 90-0353, Jan. 1990 (also, NASA TM-102437).

Komori, S., Ueda, H.,Ogino, F., and Mizushina, T., Turbulence Structure and Transport Mechanism at the Free Surface in an Open Channel Flow. Int. J. Heat Mass Trans., vol. 25, no. 4, pp. 513-521, 1982.

Launder, B.E., and Spalding, D.B., The Numerical Computation of Turbulent Flows. Comput. Methods Appl. Mech. Engr., vol. 3, no. 2, March 1974, pp. 269-289.

Lin, C.S., Numerical Studies of the Effects of Jet-Induced Mixing on Liquid-Vapor Interface Condensation. AIAA Paper 89-1744, June 1989 (also, NASA CR-182285).

Lin, C.S., and Hasan, M.M., Vapor Condensation on Liquid Surface Due to Laminar Jet-Induced Mixing: The Effects of System Parameters. AIAA Paper 90-0354, Jan. 1990 (also, NASA TM-102433).

Poreh, M, Tsuei, Y.G., and Cermak, J.E., Investigation of a Turbulent Radial Wall Jet. J. of Appl. Mech., pp. 457-463, June, 1967.

Poth, L.J., and Van Hook, J.R., Control of the Thermo-dynamic State of Space-Stored Cryogens by Jet Mixing. J. Spacecraft Rockets, vol. 9, no. 5, pp. 332-336, 1972.

Sonin, A.A., Shimko, M.A., and Chun, J.H., Vapor Condensation onto a Turbulent Liquid - I. The Steady State Condensation Rate as a Function of Liquid-Side Turbulence. Int. J. Heat Mass Trans., vol. 29, no. 9, pp. 1319-1332, 1986.

Thomas, R.M., Condensation of Steam on Water in Turbulent Motion. Int. J. Multiphase Flow, vol. 5, no. 1, pp. 1-15, 1979.

REPORT DOCUMENTATION PAGE

Form Approved
OMB No. 0704-0188

1. AGENCY USE ONLY (*Leave blank*)	2. REPORT DATE	3. REPORT TYPE AND DATES COVERED
	July 1991	Technical Memorandum

4. TITLE AND SUBTITLE

Effect of Liquid Surface Turbulent Motion on the Vapor Condensation in a Mixing Tank

5. FUNDING NUMBERS

WU-506-48

6. AUTHOR(S)

C.S. Lin, M.M. Hasan

7. PERFORMING ORGANIZATION NAME(S) AND ADDRESS(ES)

National Aeronautics and Space Administration
Lewis Research Center
Cleveland, Ohio 44135-3191

8. PERFORMING ORGANIZATION REPORT NUMBER

E-6152

9. SPONSORING/MONITORING AGENCY NAMES(S) AND ADDRESS(ES)

National Aeronautics and Space Administration
Washington, D.C. 20546-0001

10. SPONSORING/MONITORING AGENCY REPORT NUMBER

NASA TM-105555

11. SUPPLEMENTARY NOTES

Prepared for the Fourth International Symposium on Transport Phenomena in Heat and Mass Transfer sponsored by the University of New South Wales, Sydney, Australia, July 14-19, 1991. C.S. Lin, Analex Corporation, 3001 Aerospace Parkway, Brook Park, Ohio 44142 (work funded by NASA Contract NAS3-25726), and M.M. Hasan, NASA Lewis Research Center, Cleveland, Ohio. Responsible person, M.M. Hasan, (216) 433-8349.

12a. DISTRIBUTION/AVAILABILITY STATEMENT

Unclassified - Unlimited
Subject Category 34

12b. DISTRIBUTION CODE

13. ABSTRACT *(Maximum 200 words)*

The effect of liquid surface motion on the vapor condensation in a tank mixed by an axial turbulent jet is numerically investigated. The average value (over the interface area) of the root-mean-squared (rms) turbulent velocity at the interface is shown to be linearly increasing with decreasing liquid height and increasing jet diameter for a given tank size. The average rms turbulent velocity is incorporated in Brown et al. (1990) condensation correlation to predict the condensation of vapor on a liquid surface. The results are in good agreement with available condensation data.

14. SUBJECT TERMS

Liquid-vapor interface turbulence; Jet-induced mixing; Vapor condensation

15. NUMBER OF PAGES

14

16. PRICE CODE

A03

17. SECURITY CLASSIFICATION OF REPORT	18. SECURITY CLASSIFICATION OF THIS PAGE	19. SECURITY CLASSIFICATION OF ABSTRACT	20. LIMITATION OF ABSTRACT
Unclassified	Unclassified	Unclassified	

National Aeronautics and
Space Administration

Lewis Research Center
Cleveland, Ohio 44135

Official Business
Penalty for Private Use $300

FOURTH CLASS MAIL

ADDRESS CORRECTION REQUESTED

U.S.MAIL

Postage and Fees Paid
National Aeronautics and
Space Administration
NASA 451

NASA